

# A rational approach to enhancing antibody Fc homodimer formation for robust production of antibody mixture in a single cell line

Received for publication, December 8, 2016, and in revised form, August 19, 2017. Published, Papers in Press, September 6, 2017, DOI 10.1074/jbc.M116.771188

Jie Yu (于洁)<sup>†1</sup>, Xiaoxiao Wang (汪晶晶)<sup>§1</sup>, Tao Xu (须涛)<sup>§</sup>, Qiuhe Jin (金秋恒)<sup>†</sup>, Jinyuan Duan (段晋源)<sup>†</sup>, Jie Wu (吴杰)<sup>§</sup>, Haiyan Wu (吴海燕)<sup>§</sup>, Ting Xu (徐霆)<sup>§2</sup>, and Sheng Ye (叶升)<sup>†3</sup>

From the <sup>†</sup>Life Sciences Institute and Innovation Center for Cell Signaling Network, Zhejiang University, Hangzhou, Zhejiang 310058 and <sup>§</sup>Alphamab Co. Ltd., Suzhou 215125, China

Edited by Peter Cresswell

Combinations of different antibodies have been shown to be more effective for managing certain diseases than monotherapy. Co-expression of the antibody mixture in a single cell line is key to reducing complexity during antibody development and manufacturing. However, co-transfection of multiple light and heavy chains into cells often leads to production of mismatched, heterodimeric by-products that are inactive, making the development of co-expression systems that robustly and efficiently produce highly active antibody mixtures a high priority. In this study, we modified the CH3 domain interface of the antibody fragment crystallizable (Fc) region by changing several charge pairs to create electrostatic interactions favoring Fc homodimer formation and disfavoring Fc heterodimer formation. When co-expressed, these modified antibodies with altered charge polarity across the Fc dimer interface preferentially formed homodimers that fully preserved the functions of each component, rather than inactive heterodimers whose formation was reduced because of rationally designed repulsive interactions. We designed eight different combinations and experimentally screened the best one, which enabled us to produce a binary antibody mixture against the EGF receptor with a minimal heterodimer contaminant. We further determined the crystal structure of a triple-mutated Fc variant in the best combination, and we elucidated the molecular interactions favoring Fc homodimer over heterodimer formation, which provided a structural basis for further optimization. The approach presented here demonstrates the feasibility of rational antibody modification for efficient and consistent production of monoclonal antibody mixtures in a single cell line and thus broadens our options for manufacturing more effective antibody-based therapeutic agents.

During the last 2 decades, monoclonal antibodies have emerged as an important class of therapeutics for a variety of different diseases, including cancer (1, 2), autoimmune diseases (3), infectious diseases (4), and many other disorders by specifically binding to the targets, either blocking or activating certain biochemical pathways. Since 1986, more than 40 antibody products have been approved by the United States Food and Drug Administration as human therapeutics (5). It is predicted that the therapeutic antibody field will remarkably grow compared with the fields of other drug types (6). The antibody-based therapy benefits from the high mono-specificity of monoclonal antibody. For complex diseases, monoclonal antibody therapy often lacks efficacy for only binding a single molecule target. In the case of complex diseases, such as tumors, autoimmunity, and virus infection, multiple receptors or signaling pathways need to be blocked simultaneously to enhance the therapeutic efficacy (7). Antibody mixtures, which offer targeting of more than one antigen, show great advantages over antibody monotherapy (8) and are becoming a promising strategy for the treatment of different cancers and infectious diseases (9, 10).

Antibody mixtures can in principle be manufactured by two major approaches, either individually or simultaneously, with the latter one more cost-efficient. Currently, antibody mixtures can be simultaneously produced from either a single clone based on Oligoclones<sup>TM</sup> technology, in which a single cell line is transfected with a combination of IgG-encoding genes (11, 12) or by using a single batch manufacturing approach based on Sympress<sup>TM</sup> technology, in which individual stable cell lines expressing the selected antibodies are first selected and then a polyclonal cell bank is built by mixing vials of each clone together as the seed material for large scale manufacture (13–16). Both approaches allow the production of antibody mixtures in a single bioreactor; however, they are facing a number of challenges. The Oligoclones<sup>TM</sup> platform results in a mixture of a random combination of antibodies. The Sympress<sup>TM</sup> platform using multiple cell lines for generation of antibody mixtures may lead to unstable cell growth rates and antibody production. To resolve these issues, a method to efficiently and specifically express multiple monoclonal antibodies in a single cell line becomes an urgent need.

In this study, we started to express two monoclonal antibodies in a single cell line, and we encountered two issues, discrim-

This work was supported in part by Ministry of Science and Technology of China Grants 2016YFA0500404 and 2014CB910300, National Natural Science Foundation of China Grants 31525001, 31430019, and 31370721, and the Fundamental Research Funds for the Central Universities (to S.Y.). The authors declare that they have no conflicts of interest with the contents of this article. This article contains supplemental Figs. S1–S3 and Tables S1–S3.

The atomic coordinates and structure factors (code 5Y56) have been deposited in the Protein Data Bank (<http://www.pdb.org/>).

<sup>1</sup> Both authors contributed equally to this work.

<sup>2</sup> To whom correspondence may be addressed: Alphamab Co. Ltd., Suzhou 215125, China. E-mail: tingxu@alphamab.com.

<sup>3</sup> To whom correspondence may be addressed: Life Sciences Institute, Zhejiang University, 866 Yuhang Tang Rd., Hangzhou, 310058 Zhejiang, China. Tel.: 86 571 88981521; E-mail: sye@zju.edu.cn.

## Applications to antibody production

ination between the two light-chain/heavy-chain interactions and effective induction of homodimerization of the two heavy chains. The former issue can be overcome by exchange of heavy-chain and light-chain domains within the antigen-binding fragment (Fab) of one antibody (CrossMab Technology) (17). To address the latter issue, by taking advantage of the electrostatic steering mechanism (18), we rationally engineered the Fc<sup>4</sup> region of antibody by altering the charge complementarity at the Fc dimerization interface. We next screened the combinations of Fc variants that are thermally stable and efficiently promote homodimer formation with minimum contaminant of heterodimer. Based on the best scaffold, we were able to efficiently produce a binary antibody mixture against epidermal growth factor receptor (EGFR) in a single cell line with the heterodimer almost suppressed. This platform, which we called Mix-mAb, greatly extends our options to make more effective antibody agents for targeted therapies. We further determined the crystal structure of the triple mutated Fc variant of the best Fc combination, which provided the structural basis for productions and thermal stabilities of the designed Fc variants, and will allow us to design new variants for further improvement of the Mix-mAb platform.

### Results

#### *Rationale to generate monoclonal antibody mixtures in a single cell line*

A typical monoclonal antibody is “Y”-shaped and consists of two identical heavy (H) chains and two identical light (L) chains connected by disulfide bonds (Fig. 1A). The base of the Y is the Fc region and is composed of two H chains that contribute two constant domains, CH2 and CH3. The inter-molecular association between monoclonal antibody H chains in the Fc region involves extensive protein/protein interaction between the CH3 domains. The main driving force for Fc dimerization stems from the extensive interactions through the CH3 domains of the two H chains (19), which contain hydrophobic interactions, salt bridges, and disulfide bonds. The CH3 interface had been engineered to promote the formation of heterodimers of different H chains and to hinder the assembly of corresponding homodimers by changing the interactions at the CH3 domain interface (18, 20, 21). We hypothesized that the overall charge complementarity could be altered through mutagenesis of charged amino acid pairs such that attractive electrostatic interactions would favor Fc homodimer formation, whereas repulsive charged interactions would disfavor Fc heterodimer formation. This would allow two or more monoclonal antibodies to be generated in a single cell line, forming stable homodimers independently rather than heterodimers (Fig. 1B). The resulting antibody mixtures are capable of binding to different targets or multiple epitopes of the same target and thus can facilitate targeted therapies for complex diseases.

<sup>4</sup>The abbreviations used are: Fc, fragment crystallizable; EGFR, epidermal growth factor receptor; CE, capillary electrophoresis; DSC, differential scanning calorimetric; MFI, median fluorescence intensity; PDB, Protein Data Bank; H, heavy; L, light.

#### *Structure-guided rational design of the charge-pair-based Fc homodimers*

Crystal structures of the Fc region of antibodies reveal that the two subunits extensively interact through the CH3 domains, which is the main driving force for Fc dimerization. Structural comparison of a total of 48 crystal structures with coordinates corresponding to the Fc region of human IgG1 in the Protein Data Bank revealed that these structures share high similarity, especially in the interacting CH3 domains. We therefore chose a representative one (PDB code 1DN2) to identify the electrostatically interacting residues at the CH3–CH3 interface. Four independent charged residue pairs (Glu-356–Lys-439', Glu-357–Lys-370', Lys-392–Asp-399', and Asp-399–Lys-409') are highly conserved based on the sequence alignment of the CH3 domain (supplemental Fig. S1) and were chosen for further exploration (Fig. 1C). It is worth noting that due to the 2-fold symmetry present in the CH3–CH3 domain interaction, each of these residue pairs presents twice in the structure. The strategy to enhance homodimer formation by switching the charged residue polarity on the charged residue pair is schematically shown in Fig. 1D. In the wild-type Fc, the Lys-409–Asp-399' charge pair favors both heterodimer and homodimer formation. A double mutation at only one chain (K409D and D399K) preserves favorable interactions for the formation of homodimers, while leading to unfavorable repulsive interactions for the heterodimer formation. Following this strategy, we designed four basic double mutations based on the four charged residue pairs, E356K/K439E, E357K/K370E, K392D/D399K, and D399K/K409D. Because two charged residue pairs, Lys-392–Asp-399' and Asp-399–Lys-409' share the same residue Asp-399, the two designed double mutations, K392D/D399K and D399K/K409D, might have unfavorable repulsive interactions for the homodimer formation. We therefore designed a triple mutation K392D/K409D/D399K to resolve this potential problem. These variants gave rise to a total of eight different combinations in addition to the wild type (Table 1), for experimental screening of the best combination to generate monoclonal antibody mixtures through co-expression.

#### *Production and analysis of antibody mixtures generated in a single cell line*

To facilitate analysis of relative yields of homodimers and heterodimers, we chose two Fc fusions with significantly different molecular mass, a scFv-Fc fusion and a dummy Fc fragment, for co-expression in HEK293 cells and detection on non-reduced SDS-PAGE (Fig. 2A). When the two wild-type Fc fusion constructs were co-expressed, 37% of the secreted dimeric products was the scFv-Fc/Fc heterodimer (Fig. 2B and Table 1). The introduction of each basic double mutation on the Fc fragment, in combination with the wild-type scFv-Fc, only weakly increased the ratio of the homodimers (scFv-Fc/scFv-Fc and Fc/Fc) relative to the heterodimer (scFv-Fc/Fc) (Table 1 and Fig. 2B). The introduction of the triple mutation (K392D/K409D/D399K) on the Fc fragment dramatically reduced the yield of the heterodimer to only 4%, resulting in an antibody mixture predominantly containing homodimers. When addi-

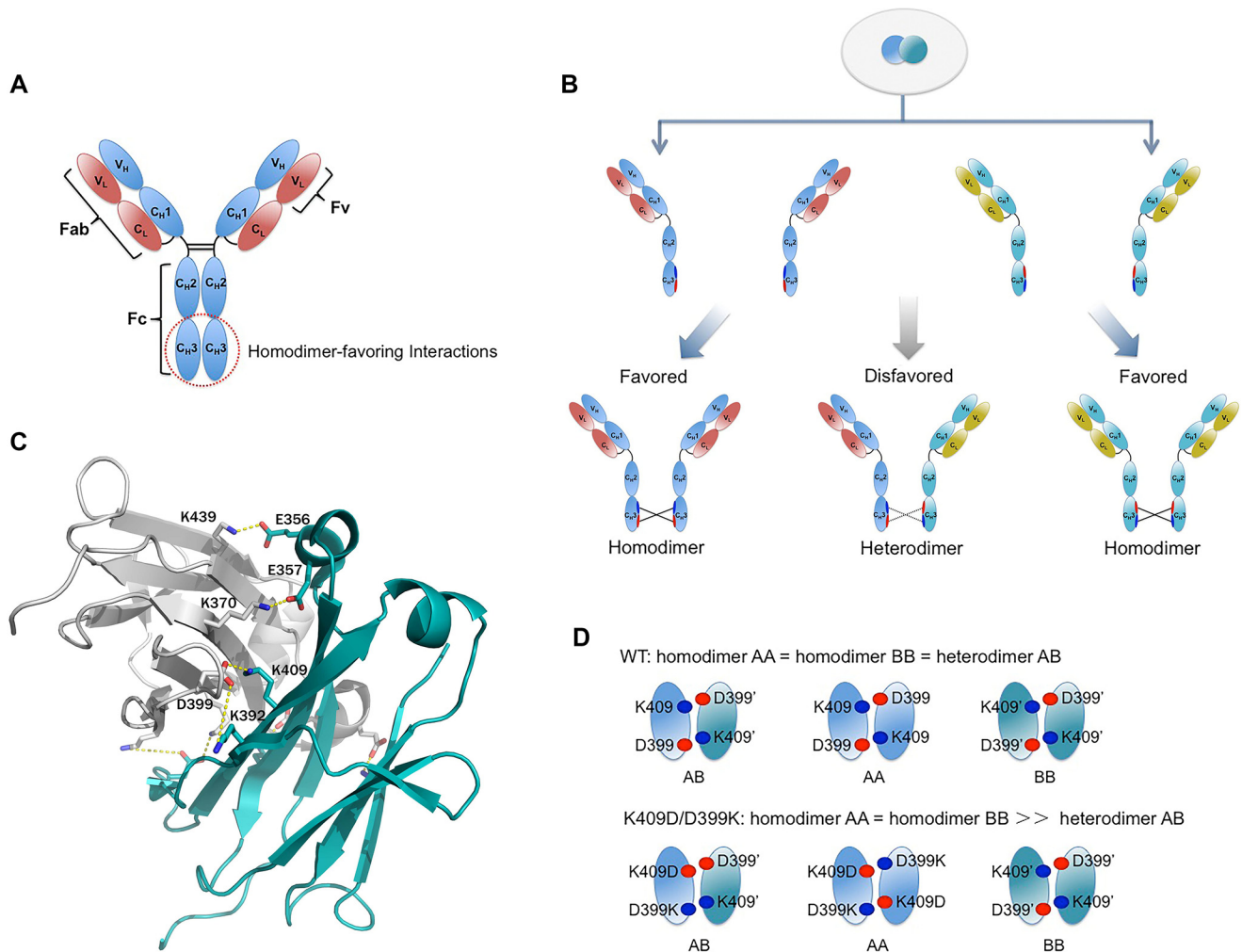


**Figure 1. Rationale to generate two or more monoclonal antibodies in a single cell line.** *A*, schematic drawing showing a typical IgG antibody. An IgG antibody is Y-shaped and consists of two H chains and two L chains. The Fab regions are located at the arms of the Y, each composed of one constant (CH1 and CL) and one variable domain (VH and VL) from each H and L chain of the antibody. The variable domains (VH and VL) form the Fv region that is important for binding to antigens. The Fc region is located at the base of the Y and is composed of two constant domains of two H chains, CH2 and CH3. The extensive protein-protein interface between CH3 domains is the main driving force for Fc dimerization, which is also the targeting interface we plan to modify for generation of monoclonal antibody mixtures in a single cell line. *B*, schematic illustrating the rationale to generate two or more monoclonal antibodies in a single cell line by altering the overall charge complementarity. *C*, crystal structure of the CH3 domain homodimer showing the four charged residue pairs. The structure is shown as *ribbon* representation with the residues shown as *sticks*. *D*, schematics showing electrostatic interactions in the wild type and charge-pair mutant as an example to enhance homodimer formation and hinder heterodimer formation. In the case of wild type, the charge/charge interaction favors both homodimer and heterodimer formation giving them equal probability. In the case of charge-pair mutant, the charge/charge interaction favors homodimer and disfavors heterodimer formation.

**Table 1**

Design of eight different combinations of ScFv-Fc and Fc variants, and the relative yields of homodimers (ScFv-Fc/ScFv-Fc and Fc/Fc) and heterodimer (ScFv-Fc/Fc)

| Combination | Variants    |                               | Relative yield (%) |            |       |
|-------------|-------------|-------------------------------|--------------------|------------|-------|
|             | scFv-Fc     | Fc                            | scFv-Fc/scFv-Fc    | scFv-Fc/Fc | Fc/Fc |
| Wild type   | None        | None                          | 25.0               | 37.0       | 38.0  |
| c1          | None        | K392D/K409D/D399K             | 44.5               | 4.2        | 51.3  |
| c2          | None        | E356K/K439E                   | 33.1               | 25.8       | 41.1  |
| c3          | None        | E357K/K370E                   | 19.9               | 32.7       | 47.5  |
| c4          | None        | E357K/K370E/K392D/K409D/D399K | 52.3               | 12.1       | 28.7  |
| c5          | E357K/K370E | K392D/K409D/D399K             | 41.5               | 5.9        | 52.6  |
| c6          | E356K/K439E | K392D/K409D/D399K             | 31.2               | 8.4        | 60.4  |
| c7          | None        | K392D/D399K                   | 36.4               | 18.9       | 44.7  |
| c8          | None        | D399K/K409D                   | 31.2               | 22.4       | 43.4  |

tional charge-pair mutations were combined with the triple mutation, either on the Fc fragment or on the scFv-Fc fusion, no further enhancement of homodimer formation was observed; instead, enhancement of heterodimer formation was observed

on these combinations. Moreover, Fc monomer formation (~6%) was observed in the antibody mixture when the pentuple mutation (E357K/K370E/K392D/K409D/D399K) was introduced on the Fc fragment, indicating that the produced anti-

## Applications to antibody production

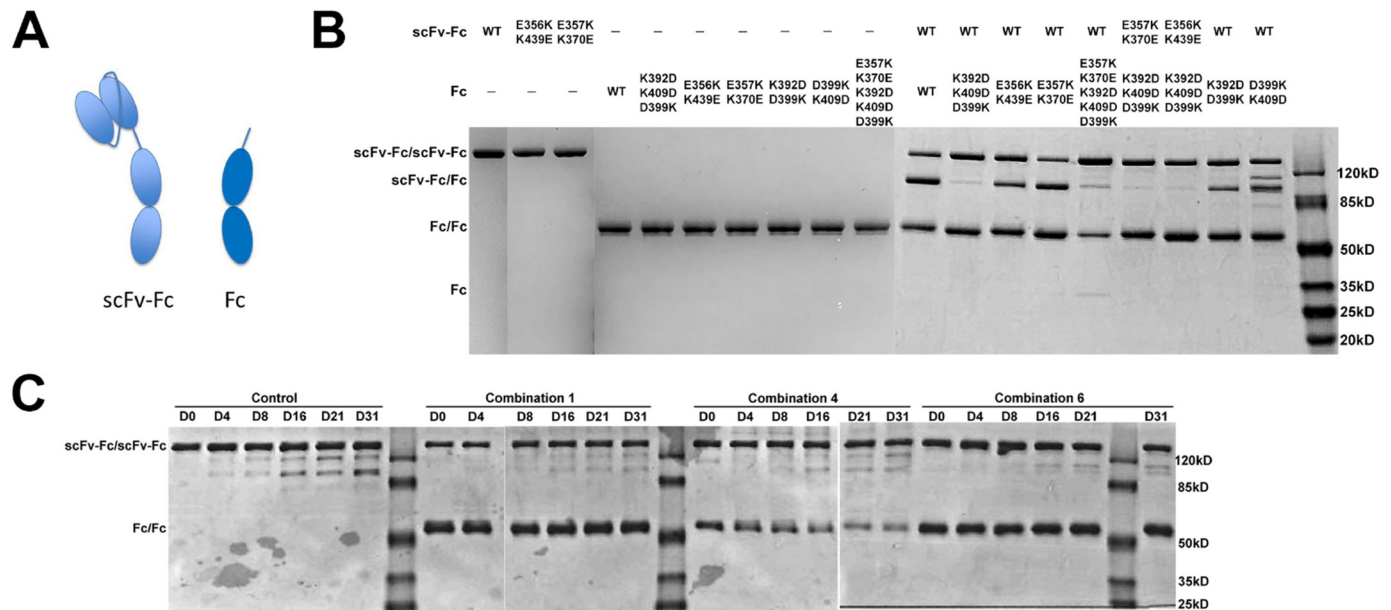


**Figure 2. Production and analysis of antibody mixtures generated in a single cell line.** A, schematic illustrating the two constructs used in the co-transfection experiments in HEK293 cells. The first construct encodes an scFv-Fc fusion with a single chain Fv attached to an Fc. The second construct encodes a dummy Fc without any attaching domain. B, products of the co-transfection experiments with different Fc variants were analyzed by SDS-PAGE under non-reduced conditions. The yields of Fc fusions are similar, and HEK293H cells always produced a little more Fc than that of scFv-Fc when the two constructs with the ratio of 1:1 were co-transfected (supplemental Table S3). The only exception is in combination 4, which contains the unstable pentuple mutation (E357K/K370E/K392D/K409D/D399K). C, thermal stability assessment at 45 °C of different Fc variants and the wild-type scFv-Fc homodimer based on SDS-PAGE analysis.

body is unstable. Overall, the results showed that three combinations (c1, c5, and c6) have the potential to be used in production of antibody mixtures in a single cell line.

It has been observed that the input DNA ratio can influence the relative proportions of the Fc dimer formation (22). To explore the influence on the relative proportions of homodimers and heterodimers in the resulting antibody mixture, we chose the best combination we obtained (triple mutation (K392D/K409D/D399K) on the Fc fragment and no mutation on the scFv-Fc) as a testing system, changed the input DNA ratio of two constructs, and analyzed the relative yields of homodimers and heterodimers (Table 2). Similar to the earlier study (22), the ratio of scFv-Fc and Fc homodimers was directly proportional to the ratio of the input DNAs. However, the proportion of scFv-Fc/Fc heterodimers remained relatively stable at ~4% with varied input DNA ratio. The data demonstrated that the input DNA ratio has little influence on the relative proportion between homodimers and heterodimers and that the triple mutation (K392D/K409D/D399K) on Fc fragment stably eliminates heterodimer formation.

### Assessment on thermal stability of generated mixtures

To determine whether the charge-pair-based designs may destabilize the antibody, we chose three representative combinations (c1, c4, and c6) in addition to the wild-type scFv-Fc homodimer for thermal stability assessment at 45 °C. As shown in Fig. 2C, wild-type scFv-Fc homodimer was reasonably stable with degraded bands showing up from the 16th day, and the scFv-Fc homodimer carrying the double mutation (E356K/K439E) was also comparably stable (combination c6). The Fc homodimer carrying the triple mutation (K392D/K409D/D399K) was highly stable without detectable degradation until

the 31st day (combinations c1 and c6). However, the Fc homodimer carrying the pentuple mutation (E357K/K370E/K392D/K409D/D399K) quickly became degraded from the 4th day. These demonstrated that the introduction of the charge-pair mutations, K392D/K409D/D399K or E356K/K439E, does not affect the thermal stability of the antibodies, whereas that of E357K/K370E/K392D/K409D/D399K dramatically reduces the thermal stability of the antibody. The antibody mixtures from combinations c1 and c6 were highly stable, similar to that of the wild type, whereas significant degradation and precipitation were observed on the antibody mixture from combination c4.

The above qualitative description is reinforced by an accurate quantitative analysis of the degradative and main peaks of each sample based on the capillary electrophoresis (CE-SDS). Each peak was integrated, and the relative proportion was calculated (Table 3). Consistent with the SDS-PAGE analysis (Fig. 2C), the degradation mainly occurred on the scFv-Fc homodimer portion starting from the 16th day. The results also showed that the antibody mixtures from combinations c1 and c6 maintained high thermal stability, indicating that the charge-pair-based design is practical.

### Production of anti-EGFR mixture using engineered Fc homodimer

EGFR is an important therapeutic target for multiple cancers (23). A number of therapeutic antibodies, including cetuximab, panitumumab, and mAb806, have been developed to target EGFR for cancer therapy. Previous studies have demonstrated that a combination of antibodies with non-overlapping epitopes for dual targeting of EGFR showed increased antitumor efficacy (24, 25).

**Table 2**  
The effects of different ratios of two co-transfected vectors on homo-/heterodimer proportions

| Combination | Variants |                   | Relative yield (%)        |                        |                 |
|-------------|----------|-------------------|---------------------------|------------------------|-----------------|
|             | scFv-Fc  | Fc                | scFv-Fc/scFv-Fc homodimer | scFv-Fc/Fc heterodimer | Fc/Fc homodimer |
| c1          | None     | K392D/K409D/D399K |                           |                        |                 |
| Ratio       | 4        | 1                 | 71.0                      | 3.8                    | 25.2            |
|             | 1        | 1                 | 44.1                      | 4.3                    | 51.6            |
|             | 1        | 4                 | 23.8                      | 4.1                    | 72.1            |

**Table 3**  
Quantitative analysis on thermal stability of antibody mixtures

| Combinations | Sample                              | 0 day             | 8th day | 21st day | 31st day |
|--------------|-------------------------------------|-------------------|---------|----------|----------|
|              |                                     | %                 | %       | %        |          |
| Wild type    | Main peak of scFv-Fc/scFv-Fc        | 99.8              | 94.5    | 85.3     | 81.2     |
|              | Degradation peak of scFv-Fc/scFv-Fc | 0.2               | 5.5     | 13.7     | 18.2     |
| c1           | Main peak of scFv-Fc/scFv-Fc        | 42.9              | 40.0    | 35.2     | 32.8     |
|              | Degradation peak of scFv-Fc/scFv-Fc | 0.4               | 4.8     | 7.9      | 8.3      |
|              | Main peak of Fc/Fc                  | 53.3              | 51.8    | 51.9     | 54.5     |
|              | Degradation peak of Fc/Fc           | 3.5               | 3.5     | 3.7      | 3.6      |
| c6           | None                                | K392D/K409D/D399K | 44.2    | 40.3     | 35.9     |
|              | Degradation peak of scFv-Fc/scFv-Fc | 0.1               | 3.8     | 4.8      | 7.4      |
|              | Main peak of Fc/Fc                  | 49.4              | 48.4    | 49.5     | 50.9     |
|              | Degradation peak of Fc/Fc           | 3.5               | 3.5     | 3.9      | 4.1      |

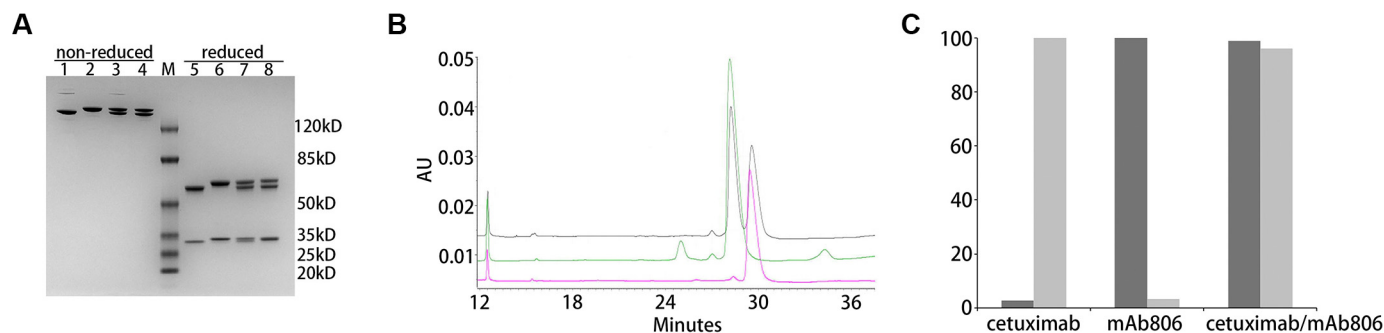


**Figure 3. Production of anti-EGFR mixture using engineered Fc homodimer.** *A*, SDS-PAGE analysis of purified cetuximab (lanes 1 and 5), mAb806 (lanes 2 and 6), cetuximab/mAb806 mixture produced *in vitro* (lanes 3 and 7), and in a single cell line (lanes 4 and 8) under both non-reduced and reduced conditions. *B*, CE-SDS analysis under non-reduced conditions of purified cetuximab (pink) and mAb806 (green), and cetuximab/mAb806 mixture (black) produced in a single cell line. The loading quantity of each sample was 100  $\mu\text{g}$ . AU indicates the UV absorption, which reflects the amount of protein passing through the capillary window. *C*, specificity detection of the cetuximab/mAb806 mixture produced in a single cell line. The y axis depicts the relative intensity of the ELISA signal. For the plates coated with EGFRVIII-D2-mFc, biotinylated EGFRVIII-D2-mFc was used as detection (dark gray), and  $A_{450}$  of mAb806 was considered as 100, whereas for that with EGFR-ECD-mFc, biotinylated EGFR-ECD-mFc was used as detection (light gray), and  $A_{450}$  of cetuximab was considered as 100.

To demonstrate the feasibility of the Mix-mAb platform, we applied the engineered Fc scaffold to produce an antibody mixture consisting of cetuximab, which binds both wild-type EGFR (WTEGFR) and a truncation form of EGFRvIII but was unable to directly inhibit the growth of EGFRvIII-expressing cells (26, 27), and mAb806, which binds to EGFRvIII and also a small portion of overexpressed WTEGFR in tumor cells (28) in a single cell line. The triple mutation K392D/K409D/D399K was introduced on the Fc fragment of cetuximab. To resolve the light chain mispairing problem, we modified mAb806 by cross-over of the CH1 and CL domains based on the CrossMab technology (17). Co-transfection of expression vectors encoding the two antibodies into HEK293F cells led to secretion of mainly two species, corresponding to two bands on SDS-PAGE under non-reduced conditions (Fig. 3A). It is worth noting that the molecular weight difference is caused by the extra glycosylation site in cetuximab (29).

We performed CE-SDS under non-reduced conditions to further characterize the produced antibody mixture. The result precisely showed that there are only two main peaks, corresponding to mAb806 and cetuximab, with proportions of 50.6

and 48.7%, respectively (Fig. 3B). We next performed bridging ELISA to detect the antibody specificities of the co-expressed product. As both cetuximab and mAb806 bind WTEGFR as well as EGFRvIII, we generated two antigens to differentiate their specificities: EGFRvIII-D2-mFc, in which EGFR residues Asn-274–Ile-332 are fused to mouse IgG1 Fc, only interacts with mAb806; and EGFR-ECD-mFc, in which EGFR residues Leu-1–Ser-621 are fused to mouse IgG1 Fc, mainly interacts with cetuximab while hardly recognized by mAb806. The results indicated that cetuximab/mAb806 mixture produced in a single cell line has two different specificities, each of them was similar to the binding specificity of cetuximab or mAb806 (Fig. 3C).

The produced antibody mixture was further examined by FACS analysis for binding to tumor cell surface-expressed EGFR. We used three different tumor cells in the study, U87MG cells with overexpressed EGFRvIII (U87MG-EGFRvIII), and A431 cells or CNE cells, both overexpressing WTEGFR. When U87MG-EGFRvIII cells were probed with individually produced cetuximab or mAb806 in four different concentrations (0.1, 1, 10, or 100  $\mu\text{g ml}^{-1}$ ), or their mixture was

## Applications to antibody production

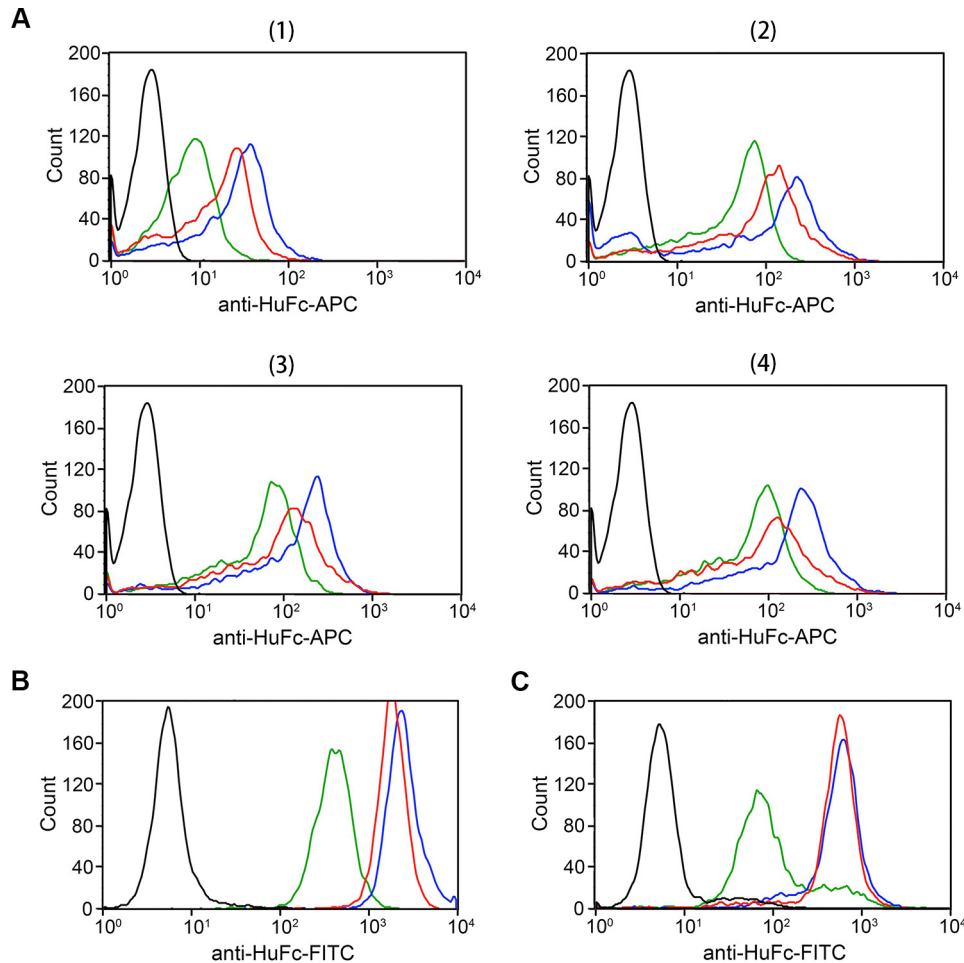


**Figure 4. Flow cytometric analysis of U87MG-EGFRvIII (A), A431 (B), and CNE (C) cell lines.** Cells were stained with an irrelevant isotype control (black), mAb806 (green), cetuximab (red), and cetuximab/mAb806 mixture (blue). A, panels 1–4, U87MG-EGFRvIII cells were probed with individually produced mAb806 (green) or cetuximab (red) in four different concentrations (0.1, 1, 10, or 100  $\mu\text{g ml}^{-1}$ ), or their mixture (blue) was produced in a single cell line, also in four different concentrations (0.2, 2, 20, or 200  $\mu\text{g ml}^{-1}$ ). B and C, either A431 or CNE cells were probed with individually produced cetuximab or mAb806 in a saturated concentration (100  $\mu\text{g ml}^{-1}$ ) or with the cetuximab/mAb806 mixture produced in a single cell line in a saturated concentration (200  $\mu\text{g ml}^{-1}$ ).

**Table 4**  
Flow cytometric analysis of U87MG-EGFRvIII, A431 and CNE cell lines

| Cell line      | Concentration<br>$\mu\text{g/ml}$ | MFI       |        |  |
|----------------|-----------------------------------|-----------|--------|--|
|                |                                   | Cetuximab | mAb806 | Antibody mixture<br>(2 $\times$ concentration) |
| U87MG-EGFRvIII | 0.1                               | 24.6      | 14.5   | 34.6   |
|                | 1                                 | 101.6     | 53.7   | 148.1  |
|                | 10                                | 100.2     | 63.5   | 144.1  |
|                | 100                               | 95.5      | 70.0   | 174.4  |
| A431           | 100                               | 1765.1    | 224.9  | 1813.0   |
| CNE            | 100                               | 464.3     | 99.2   | 492.2  |

produced in a single cell line, also in four different concentrations (0.2, 2, 20, or 200  $\mu\text{g ml}^{-1}$ ) (Fig. 4 and Table 4), the median fluorescence intensity (MFI) of the cetuximab/mAb806 mixture is approximately equal to the addition of the MFIs of cetuximab and mAb806 in all four different concentrations (Table 4), indicating that cetuximab and mAb806 can simultaneously bind to different epitopes of a single EGFRvIII molecule. When either A431 or CNE cells were probed with individually produced cetuximab or mAb806 in a saturated concentration (100  $\mu\text{g ml}^{-1}$ ) (Fig. 4, B and C, and Table 4), the resulting MFIs of cetuximab were significantly higher than those of mAb806. This was expected because mAb806 only binds  $\sim 10\%$  WTEGFR

(28), whereas cetuximab binds to all WTEGFR (27). When either A431 or CNE cells were probed with the cetuximab/mAb806 mixture produced in a single cell line in a saturated concentration (200  $\mu\text{g ml}^{-1}$ ), the MFIs are only slightly higher than those of cetuximab, indicating that mAb806 in the mixture binds to only a small portion of WTEGFR. Taken together, the FACS data demonstrate that the cetuximab/mAb806 mixture produced in a single cell line has the same efficacy compared with the mixture from two individually produced antibodies.

We further examined the antitumor activity of the cetuximab/mAb806 mixture in glioma tumor xenografts. Treatment

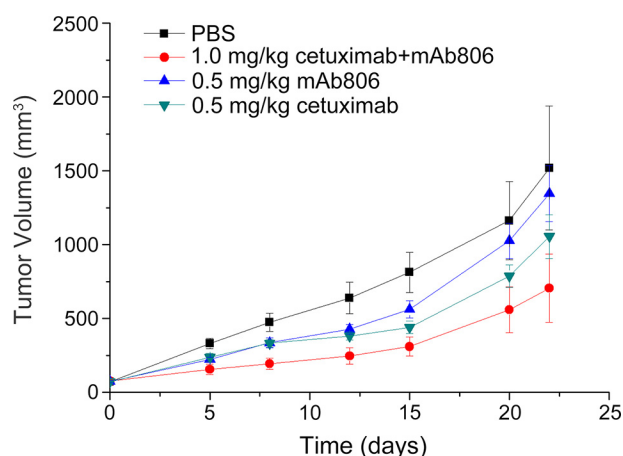


**Figure 5. Treatment of established U87MG-EGFRvIII xenografts with mAb806, cetuximab, and cetuximab/mAb806 mixture.** Mice ( $n = 6$ ) bearing U87MG-EGFRvIII xenografts were injected i.p. with PBS (■), 0.5 mg/kg mAb806 (▲), 0.5 mg/kg cetuximab (▼), or 1 mg/kg cetuximab/mAb806 mixture (●), three times weekly for 2 weeks.

of established U87MG-EGFRvIII glioma xenografts with 1.0 mg/kg cetuximab/mAb806 mixture produced in a single cell line, in which cetuximab and mAb806 are both  $\sim 0.5$  mg/kg, displayed higher antitumor activity than either antibody alone (Fig. 5). At day 22 after tumor inoculation, the U87MG glioma xenograft treated with cetuximab/mAb806 mixture had a mean tumor volume of  $704 \text{ mm}^3$ , which was significantly lower than those treated with vehicle ( $1519 \text{ mm}^3$ ), cetuximab alone ( $1054 \text{ mm}^3$ ), and mAb806 alone ( $1346 \text{ mm}^3$ ). Furthermore, treatment with cetuximab/mAb806 mixture caused 53% tumor growth inhibition, greater than additive antitumor activity of mAb806 alone and cetuximab alone.

### Crystal structure of the triple-mutated Fc homodimer

To elucidate the molecular interactions favoring Fc homodimer formation over the heterodimer, we sought to solve the crystal structure of the Fc homodimer carrying the triple mutation (K392D/K409D/D399K). The Fc homodimer was purified from mammalian HEK293F cell cultures after transient transfection of the plasmid carrying the triple-mutated Fc fragment. Well-diffracting crystals were obtained through micro-seeding. The crystals belong to space group  $P6_522$  with unit-cell dimensions of  $a = 65.1 \text{ \AA}$  and  $c = 477.6 \text{ \AA}$ . The asymmetric unit consists of two chains forming an Fc homodimer. The structure was determined by the molecular replacement method. The current model, refined at a resolution of  $2.65 \text{ \AA}$ , has a crystallographic  $R$  value of 26.0% and an  $R_{\text{free}}$  of 29.8%. The electron densities of carbohydrates attached to the glycosylation site of the Asn-297 residues in Fc could be clearly resolved. The model has good geometry (Table 5), and 100% of the non-glycine backbone dihedral angles are in the most favored or allowed regions.

The triple-mutated Fc exists as a homodimer in the crystal, in agreement with the data from production and thermal stability assessment of antibody mixtures. Each Fc chain contains two constant domains (CH2 and CH3) connected by a linker. The structure of the triple-mutated CH3 domain is identical to that of the wild-type one (PDB code 1DN2), with a root mean squared deviation (RMSD) of  $0.4 \text{ \AA}$  for all  $C\alpha$  atoms of the CH3 domain (residues 341–443), indicating that the triple mutation

**Table 5**  
X-ray data and refinement statistics

|                                       |   |
|---------------------------------------|---|
| <b>Data collection</b>                |   |
| Space group                           | $P6_522$  |
| Unit cell                             | $a = 65.1 \text{ \AA}$ ,<br>$c = 477.6 \text{ \AA}$ |
| Resolution ( $\text{\AA}$ )           | 2.65  |
| Measured reflections                  | 584,843   |
| Unique reflections                    | 18,054  |
| Redundancy                            | 13.1  |
| Completeness (% (highest shell))      | 95.4 (97.9)   |
| Mean $I/\sigma$ (highest shell)       | 50.6 (2.3)  |
| $R_{\text{sym}}$ (% (highest shell))  | 0.107 (0.000)                                       |
| <b>Refinement</b>                     |   |
| Resolution ( $\text{\AA}$ )           | 2.65  |
| No. of reflections $ F  > 0 \sigma F$ | 18,043  |
| $R$ -factor/ $R$ -free (%)            | 26.0/29.8   |
| No. of atoms                          |   |
| Protein                               | 3,323   |
| Carbohydrate                          | 196   |
| Water                                 | 94  |
| Root mean square deviations           |   |
| Bond lengths ( $\text{\AA}$ )         | 0.009   |
| Bond angles ( $^\circ$ )              | 1.176   |
| Ramachandran plot                     |   |
| Most favored regions (%)              | 95.4  |
| Additional allowed regions (%)        | 3.1   |
| Generously allowed regions (%)        | 0.5   |
| Disallowed regions (%)                | 0.0   |

introduced on the CH3 domain does not change the domain structure. However, we observed substantial differences in the dimer interface between the two CH3 domains. As shown in Fig. 6A, two CH3 subunits interacting through the dimer interface undergo an  $\sim 9^\circ$  rotation relative to each other between triple-mutated and wild-type Fc dimers. In the wild-type Fc dimer, three electrostatically interacting charge pairs (Glu-357–Lys-370', Lys-409–Asp-399', and Lys-392–Asp-399') at the dimerization interface are closed in space (Fig. 6B). Among the three charge pairs, two of them (Glu-357–Lys-370' and Lys-409–Asp-399') interact strongly, and the third one (Lys-392–Asp-399') interacts weakly, as evidenced by the flipping away of the side chain of Lys-392. Although in the triple-mutated Fc dimer, these residues form a charge network, including four charge pairs (Glu-357–Lys-370', Lys-370'–Asp-409, Asp-409–Lys-399', and Lys-399–Asp-392') (Fig. 6C). Replacement of three independent charge pairs with a charge network, including four strongly interacting charge pairs has two structural consequences: (i) stabilization of the triple-mutated Fc dimer structure and (ii) facilitation of the  $9^\circ$  relative rotation of the two CH3 subunits interacting through the dimer interface. Because of the 2-fold symmetry present in the CH3–CH3 domain interaction, the triple-mutated Fc dimer has two additional and two stronger charge pairs, in comparison with the wild-type one, thereby dramatically reducing the free energy. Furthermore, the formation of the new charge network at the rim of the CH3–CH3 interface slightly twists the two CH3 domains, leaving the  $C\alpha$  atom of residue 399 shifted by  $1.8 \text{ \AA}$ .

### Discussion

In recent years, enhancing the efficacy of antibody-based therapies has been the subject of intense investigation. Recombinant antibody mixtures, as an important new class of antibody therapeutics, have attracted more and more attention as a treatment of complex diseases (9, 10). Evidence from both pre-clinical and clinical trials suggests that combinations of anti-

## Applications to antibody production

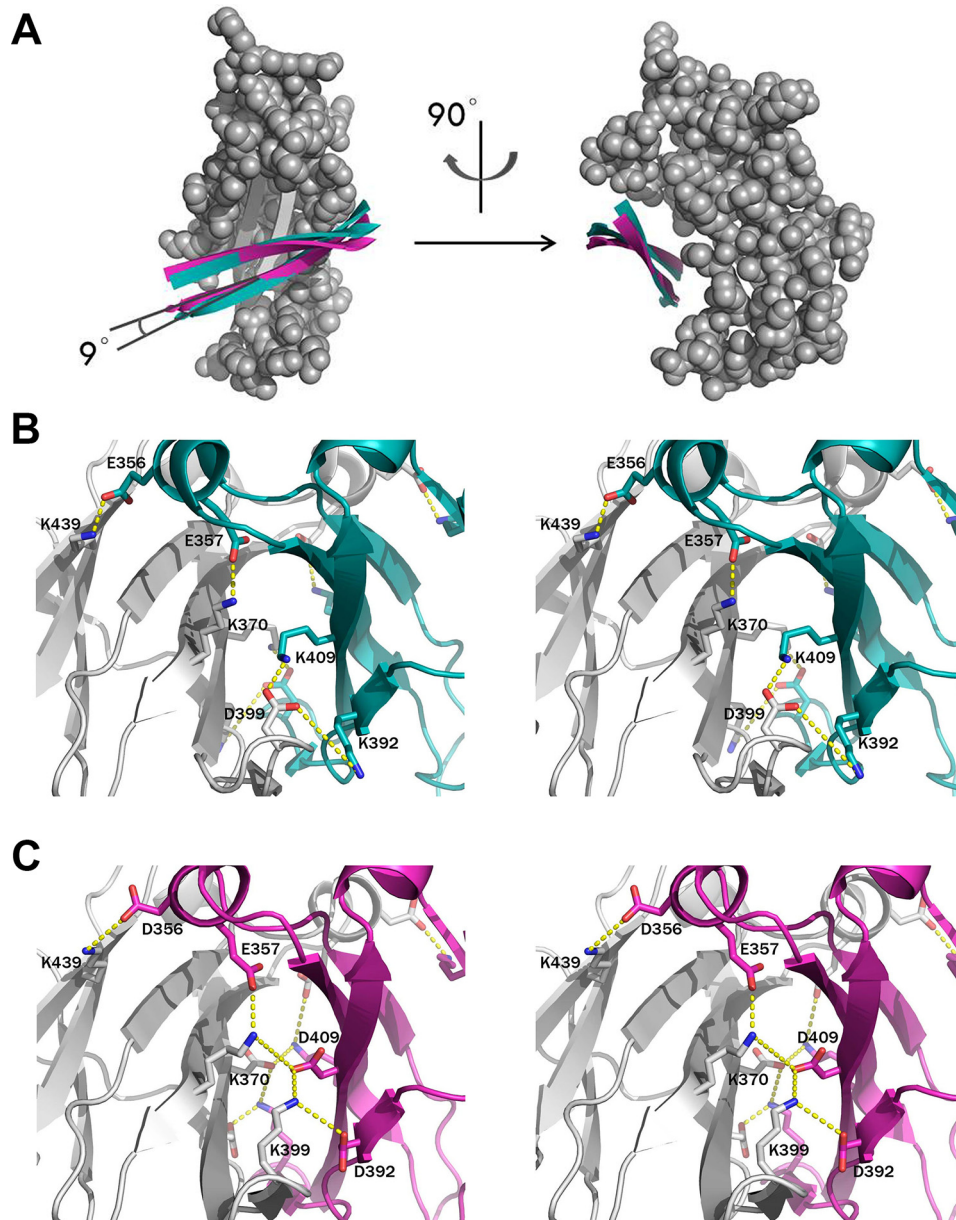


**Figure 6. Crystal structure of the triple-mutated Fc homodimer reveals a relative rotation and a charge network formation.** A, relative rotation between two CH3 subunits at the dimer interface. One CH3 subunit is in gray CPK representation. Only two  $\beta$ -strands are shown in the other subunit, as cyan ribbons in the wild type and maroon in the triple-mutated Fc homodimers. B and C, stereoviews of the interdimer interactions in the wild type (B) and the triple-mutated (C) Fc dimer.

bodies specific to non-overlapping epitopes on the same target or distinct targets can increase the efficacy over individual monoclonal antibodies. As an example, Sym004, which was recently developed by Symphogen, is a 1:1 mixture of two chimeric antibodies (mAb992 and mAb1024) against non-overlapping epitopes on the extracellular domain of EGFR (24). This antibody mixture possesses a unique mechanism of action that induces rapid EGFR internalization and subsequent degradation of internalized receptors by EGFR cross-linking (24). In preclinical studies, Sym004 worked highly synergistically compared with anti-EGFR monoclonal antibodies (24, 30). These observations certified the potential of Sym004 to treat tumors with acquired resistance to EGFR-targeted agents, and the phase II trials to evaluate the clinical activity of Sym004 are currently ongoing.

Several strategies have been developed for generation of antibody mixtures. First, two or more individual mAbs are generated as individual drug products and are then administered to the patients at the same time (31). Second, monoclonal antibodies are individually generated as drug substances and subsequently mixed into one drug product (24). Third, using Oligoclomics<sup>TM</sup> technology, one common light chain and multiple heavy chains are co-transfected into a single cell line, allowing two or more antibodies simultaneously produced in a single cell line (12). Fourth, based on the Sympress<sup>TM</sup> technology, antibody mixtures can be produced by single-batch manufacturing in a single polyclonal master cell bank containing multiple cell lines (14). The first two strategies mixing separately generated antibodies may not be commercially viable due to prohibitive increases in cost and time. Although simultaneous manu-

facturing of recombinant antibody mixtures is more cost-efficient, current approaches based on either Oligoclones™ or Sympress™ technologies face challenges. Using the Oligoclones™ technology, the resulting antibody mixtures via a single cell line include both monospecific and bispecific antibodies, which may greatly increase product complexity and give challenges in clone stability and manufacturing consistency (32). Using Sympress™ technology, large numbers of cell lines that each stably express the selected antibody are required to generate, and multiple cell lines for antibody mixture production may inevitably lead to different cell growth characteristics and asymmetrical contribution of individual mAbs to the eventual mixture and probably batch-to-batch variations. The objective of this study was to develop a new technology that produces a mixture of multiple different antibodies in a single cell line. By taking advantage of the electrostatic steering mechanism, we designed several charge pairs by altering the overall charge complementarity on the CH3 domain interface of the antibody Fc region and screened the best combination that forms stable homodimers independently rather than a heterodimer. These Fc variants maintained high thermal stability and allowed us to produce an antibody mixture against EGFR with minimal heterodimer contaminants in combination with the CrossMab technology (17). The results of this study demonstrate that two monoclonal antibodies can be effectively and specifically produced in a single cell line to form stable homodimers independently rather than a heterodimer.

In a pioneering study, an electrostatic steering mechanism was used to engineer the CH3 domain interface for Fc heterodimerization (18). Through screening many designed variants, they have determined that the combination of two pairs of charge mutations (K409D-K392D/D399K-E356K) on two respective Fc chains at the CH3 interface produced predominantly Fc heterodimers without reduced yield (18). In this study, we applied an electrostatic steering mechanism to promote Fc homodimerization. After a survey of many variants, we have determined that a triple-mutated (K392D/K409D/D399K) Fc form stable homodimers independently rather than a heterodimer when co-expressed with wild-type Fc. However, the structural basis underlying different productivities and thermal stabilities is unclear. We further determined the crystal structure of the triple-mutated Fc dimer, which provides us plausible explanations for the productivity and thermal stability of antibody mixtures generated in a single cell line. Simple alteration of the charge complementarity of a charged amino acid pair by the introduction of a basic double mutation on the Fc fragment generates an attractive electrostatic interaction favoring Fc homodimer formation as we hypothesized. However, the alteration might also cause relative rotation of the two CH3 subunits interacting through the dimer interface, which might increase the free energy and counteract the attractive electrostatic interaction, thus disfavoring Fc homodimer formation. This explains the weakly increased formation of a homodimer than that of a heterodimer by the introduction of each basic double mutation on the Fc fragment in combination with the wild-type scFv-Fc. The introduction of the triple mutation (K392D/K409D/D399K) on the Fc fragment generates a charge network, including four strongly interacting charge

pairs, which dramatically increases the thermal stability of Fc homodimer, thus favoring Fc homodimer formation. However, combination of an additional charge-pair mutation with the triple mutation breaks the charge network on the triple-mutated Fc fragment and therefore reduces Fc homodimer formation.

The relative rotation of the two CH3 subunits observed in the crystal structure raises the following obvious concerns regarding the engineered Fc: whether it could lead to lower stability thus reducing its serum half-life, or whether it could affect Fc interactions with Fc receptors therefore impacting its effector functions. The differential scanning calorimetric (DSC) profiles (supplemental Fig. S2) revealed a lower melting temperature ( $T_m$ ) of 68 °C for the triple-mutated (K392D/K409D/D399K) Fc than that (~83 °C) for wild-type Fc. Similarly reduced  $T_m$  was observed on an engineered Fc heterodimer using an electrostatic steering mechanism relative to that of WT (18), indicating that changing structurally conserved residues in the CH3-CH3 interface may lead to lower  $T_m$ . However, our qualitative comparison of DSC profiles revealed similar  $T_m$  values between the triple-mutated Fc homodimer and the engineered Fc heterodimer from a prior study (18), and it suggested that the  $T_m$  is still well within a range that will support viable therapeutic protein productions, as suggested by our accelerated stability test (Fig. 2C) and the prior study (18). To determine the interactions between the triple-mutated (K392D/K409D/D399K) Fc and Fc receptors, we further performed ELISAs with two Fc receptors (FcγRIIa and FcγRIIIa176V) closely related to effector functions (supplemental Fig. S3), and we showed that the triple-mutated Fc has similar affinities to Fc receptors relative to those of wild-type Fc, which is expected, as the co-crystal structure of Fc and Fc receptor shows that Fc interacts with Fc receptor through its CH2 domain, which is linked to CH3 domain via a flexible linker (33). Thus, the subtle rotation of the two CH3 subunits will likely be compensated by the relative movement between CH2 and CH3 domains, without impact on the interactions between Fc and Fc receptors.

Our current Mix-mAb platform allows us to specifically produce two monoclonal antibodies in a single cell line. However, antibody mixtures may contain three or more different antibodies. As an example, an anti-botulinum neurotoxin product contains three different antibodies (34). Although our studies revealed three different combinations (Table 1) available to produce antibody mixtures containing two different antibodies, a simple combination of any three variants will obviously lead to mismatched by-products. To produce three or more monoclonal antibodies in a single cell line, the current Mix-mAb platform needs further improvement. Toward this purpose, the crystal structure of the triple-mutated Fc dimer not only provided us explanations for current data of the production of antibody mixtures, but also can serve as a starting structure to design and screen new variants for generation of antibody mixtures in a single cell line.

## Conclusions

In conclusion, we have developed a Mix-mAb platform, in which the charged residues around the rim of the CH3 domain interface were engineered to effectively suppress heterodimer

## Applications to antibody production

formation. Based on this platform, we have successfully produced anti-EGFR antibody mixture in a single cell line. Furthermore, we determined the crystal structure of the triple-mutated Fc variant of the best Fc combination, which will allow us to further improve the Mix-mAb platform for antibody mixtures production, as well as their clinical potential.

### Experimental procedures

#### Computational analyses

Our structural analysis of a total of 48 crystal structures of the Fc region of human IgG1 from the Protein Data Bank revealed that these antibody structures share high similarity, especially in the CH3 domain. We chose one of them, a Fc fragment of human IgG1 (PDB code 1DN2) (35), for the following study. To identify the interface residues in the CH3 domain that may influence Fc dimerization, a method called Contact Map Analysis, based on the distance between amino acid side-chain non-hydrogen atoms and the non-hydrogen atoms of any residues in the second chain, was used here. A total of 34 interfacial residues (supplemental Table S1) were identified using the distance limit of 4.5 Å, among which there are eight charged residue pairs (supplemental Table S2). These residues are highly conserved between different IgG subclasses from humans or mice (supplemental Fig. S1).

#### Construct generation

Genes of human IgG1 Fc and fusion protein scFv-Fc were cloned into pcMVβ and pcDNA3.1-zeo mammalian expression vectors, respectively. Different mutations of the charged residue pairs were introduced on either Fc or scFv-Fc with the negative-charged amino acids (Asp and Glu) to the positive-charged ones (Lys, Arg, and His) or the positive-charged amino acids to the negative-charged ones. The mutations were generated using the QuikChange site-directed mutagenesis kit (Agilent Technologies) and verified by DNA sequencing. We chose eight combinations of Fc and scFv-Fc variants (Table 1) for the subsequent experiments.

#### Protein production and analysis

The two constructs with the ratio of 1:1 were co-transfected into suspended HEK293H cell culture using Lipofectamine 2000 reagent or polyethyleneimine. The cell culture supernatant was harvested 3–4 days later after transfection. Proteins were purified by immunoprecipitation using protein A-agarose resin and run on non-reduced SDS-polyacrylamide gels. The gels were then analyzed using the professional imaging analysis software Gel-Pro to examine the relative proportion of homodimers (Fc/Fc and scFv-Fc/scFv-Fc) and heterodimer (scFv-Fc/Fc) in the produced mixtures. To investigate the influence of different ratios of input DNA on homodimer and heterodimer formation, we co-transfected the two constructs in combination c1, respectively, in ratios of 4:1, 1:1, and 1:4, into suspension-cultured 293H cells.

#### Thermal stability assessment

Each antibody mixture at a concentration of 10 mg/ml in a 25 mM sodium citrate, 250 mM sodium chloride aqueous buffer at

pH 8.5 was incubated at 45 °C for a period of 31 days. At discrete time points, sample aliquots were removed and analyzed by SDS-PAGE and CE-SDS.

#### CE-SDS

The CE-SDS was performed using a Beckman P/ACE system with a 50-cm × 75-μm inner diameter uncoated fused-silica capillary. The mobile phase was 12 mM sodium borate buffered to pH 9.4 containing 25 mM SDS. After pressure injection, the separation was performed at 30 kV for 8 min at 25 °C and monitored at 214 nm. Lyophilized samples were diluted with water to a concentration of 1 mg/ml prior to injection. Neutral species were determined to migrate at 2.3 min.

#### Generation of antibody mixture against EGFR

The genes of cetuximab and mAb806 were constructed into mammalian expression vectors pcDNA4.0, respectively, with the triple mutation K392D/K409D/D399K introduced on the Fc region of cetuximab. In the meantime, a CrossMab version of mAb806 was generated, as described previously (17), to prevent the mis-match of two different light chains. Proteins were then co-expressed in HEK293 cells and purified according to the methods as mentioned above.

#### ELISA

ELISA for detection of the co-expressed product consisting of two different antibody specificities was performed as follows. Antigens were coated at 2 or 3 μg/ml in 96-well plates. Plates were blocked at room temperature for 2 h. The samples (25 μg/ml) and the respective biotinylated antigens were then added. After incubation for 2 h, plates were developed using streptavidin-HRP. The absorbance values were read at 450 nm. ELISA for determination of the interactions between the triple-mutated Fc and Fc receptors was performed as follows. The 96-well plates were coated with wild-type Fc or triple-mutated (K392D/K409D/D399K) Fc at 2 μg/ml. After overnight incubation at 4 °C, the plates were blocked with 3% BSA at room temperature for 2 h. Then serial dilution of His-tagged FcγRIIIa and FcγRIIIa176V (1,000,000 to 0.954 ng/ml) were added and incubated for 1 h at room temperature. Bound receptors were detected using an HRP-conjugated anti-His antibody. The absorbance values were read at 450 nm.

#### Fluorescence-activating cell sorter (FACS) analysis

Three different cell lines were used for FACS analysis: 1) U87MG-EGFRvIII, human glioblastoma cell line U87MG (expressing low levels of endogenous WTEGFR) transfected with the EGFRvIII gene; 2) A431, human squamous carcinoma cell line A431 (expressing high levels of WTEGFR); and 3) CNE, human nasopharyngeal carcinoma cell line CNE (expressing high levels of WTEGFR).

Approximately  $1 \times 10^6$  U87-EGFRvIII cells, A431 cells, or CNE cells were incubated with various antibodies at 4 °C for 30 min, following by incubation with rabbit anti-human IgG-fluorescein isothiocyanate conjugate (FITC) for an additional 30 min. After several washes with cold PBS, the cells were analyzed by a flow cytometer (model GUAVA®, Merck) The data were

acquired, and the median fluorescence intensities (MFI) were calculated by Guava 5.3.1.

### Differential scanning calorimetry

DSC was performed on a MicroCal VP-capillary DSC (GE Healthcare). Measurements were carried out for all samples at a concentration of 2 mg/ml in PBS buffer (pH 7.4). Each sample was heated from 25 to 110 °C at a rate of 95 °C/h. The thermogram was fitted using  $C_p$  value versus temperature after deduction of the PBS buffer reference scan.

### Xenograft models

Six- to seven-week-old female BALB/c Nude mice were purchased from Charles River Laboratories (Wilmington, MA) and acclimated for 1 week upon delivery. Each mouse was injected s.c. into the right flank with  $2 \times 10^6$  U87MG-EGFRvIII cells (U87MG-EGFRvIII cell line constantly expressing human EGFRvIII protein) in 50% culture medium and 50% Matrigel (BD Biosciences). Tumor volumes were calculated as  $\pi/2 (L \times W^2)$ , where  $L$  is the longest diameter measured with calipers, and  $W$  is the diameter perpendicular to  $L$ . When the mean tumor volume reached  $\sim 100 \text{ mm}^3$ , mice were randomized by tumor volume into treatment group, and tumor volume was recorded twice weekly thereafter. Statistical analyses were performed by using GraphPad Prism version 5.01 software (San Diego). Data are expressed as means  $\pm$  S.E. of three independent experiments. Two group comparisons were performed by using unpaired Student's  $t$  test. Multiple group comparisons were performed by one-way analysis of variance followed by Dunnett's  $t$  test.

### Crystallization and data collection

The purified triple-mutated Fc fragment was concentrated to  $\sim 10 \text{ mg/ml}$  for crystallization. Crystals were grown by sitting drop vapor diffusion at 20 °C by mixing equal volumes of protein and reservoir solution of 1.5 M  $(\text{NH}_4)_2\text{SO}_4$ , 10% glycerol, 0.1 M Tris-HCl (pH 7.5). Initial crystallization only produced stacking plates containing multiple crystals. Well-diffracting crystals were obtained through micro-seeding.

Crystals were cryo-protected from the mother liquid by increasing the concentration of glycerol to 35% before flash-freezing in liquid nitrogen. Diffraction data were collected at Shanghai Synchrotron Facility (SSRF) BL17U beam line. The data were indexed, integrated, and scaled using the program HKL-2000 (36).

### Structure determination and refinement

The crystals belong to space group  $P6_522$  with unit-cell dimensions of  $a = 65.1 \text{ \AA}$  and  $c = 477.6 \text{ \AA}$  and contained an Fc dimer in one asymmetric unit. Phases were determined by molecular replacement using PHASER (37) with the Fc structure (PDB code 1DN2) as a search model. Model adjustment was done iteratively using Xtalview (38), and structure refinement was done using REFMAC (39). The models were refined with data to a resolution of 2.65 Å, maintaining highly restrained stereochemistry and keeping tight non-crystallographic symmetry restraints (Table 5). All structural illustrations were prepared with PyMOL (40).

**Author contributions**—S. Y. and T. X. designed the study. J. Y., X. W., T. X., J. W., and H. W. designed, performed, and analyzed the experiments shown in Figs. 1–5. J. Y., T. X., J. D., Q. J., and S. Y. designed, performed, and analyzed the experiments shown in Fig. 6. All authors analyzed the results and approved the final version of the manuscript.

### References

- Weiner, L. M., Surana, R., and Wang, S. (2010) Monoclonal antibodies: versatile platforms for cancer immunotherapy. *Nat. Rev. Immunol.* **10**, 317–327
- Scott, A. M., Wolchok, J. D., and Old, L. J. (2012) Antibody therapy of cancer. *Nat. Rev. Cancer* **12**, 278–287
- Chan, A. C., and Carter, P. J. (2010) Therapeutic antibodies for autoimmunity and inflammation. *Nat. Rev. Immunol.* **10**, 301–316
- Casadevall, A., Dadachova, E., and Pirofski, L. (2004) Passive antibody therapy for infectious diseases. *Nat. Rev. Microbiol.* **2**, 695–703
- Ecker, D. M., Jones, S. D., and Levine, H. L. (2015) The therapeutic monoclonal antibody market. *MAbs* **7**, 9–14
- Nelson, A. L., Dhimolea, E., and Reichert, J. M. (2010) Development trends for human monoclonal antibody therapeutics. *Nat. Rev. Drug Discov.* **9**, 767–774
- Beck, A., Wurch, T., Bailly, C., and Corvaia, N. (2010) Strategies and challenges for the next generation of therapeutic antibodies. *Nat. Rev. Immunol.* **10**, 345–352
- Raju, T. S., and Strohl, W. R. (2013) Potential therapeutic roles for antibody mixtures. *Expert Opin. Biol. Ther.* **13**, 1347–1352
- Demarest, S. J., Hariharan, K., and Dong, J. (2011) Emerging antibody combinations in oncology. *MAbs* **3**, 338–351
- Marasco, W. A., and Sui, J. (2007) The growth and potential of human antiviral monoclonal antibody therapeutics. *Nat. Biotechnol.* **25**, 1421–1434
- de Kruif, J., Kramer, A., Nijhuis, R., van der Zande, V., den Blanken, R., Clements, C., Visser, T., Keehnen, R., den Hartog, M., Throsby, M., and Logtenberg, T. (2010) Generation of stable cell clones expressing mixtures of human antibodies. *Biotechnol. Bioeng.* **106**, 741–750
- Logtenberg, T. (2007) Antibody cocktails: next-generation biopharmaceuticals with improved potency. *Trends Biotechnol.* **25**, 390–394
- Frandsen, T. P., Naested, H., Rasmussen, S. K., Hauptig, P., Wiberg, F. C., Rasmussen, L. K., Jensen, A. M., Persson, P., Wikén, M., Engström, A., Jiang, Y., Thorpe, S. J., Förberg, C., and Tolstrup, A. B. (2011) Consistent manufacturing and quality control of a highly complex recombinant polyclonal antibody product for human therapeutic use. *Biotechnol. Bioeng.* **108**, 2171–2181
- Wiberg, F. C., Rasmussen, S. K., Frandsen, T. P., Rasmussen, L. K., Tengbjerg, K., Coljee, V. W., Sharon, J., Yang, C. Y., Bregenholt, S., Nielsen, L. S., Haurum, J. S., and Tolstrup, A. B. (2006) Production of target-specific recombinant human polyclonal antibodies in mammalian cells. *Biotechnol. Bioeng.* **94**, 396–405
- Nielsen, L. S., Baer, A., Müller, C., Gregersen, K., Mønster, N. T., Rasmussen, S. K., Weilguny, D., and Tolstrup, A. B. (2010) Single-batch production of recombinant human polyclonal antibodies. *Mol. Biotechnol.* **45**, 257–266
- Rasmussen, S. K., Rasmussen, L. K., Weilguny, D., and Tolstrup, A. B. (2007) Manufacture of recombinant polyclonal antibodies. *Biotechnol. Lett.* **29**, 845–852
- Schaefer, W., Regula, J. T., Böhner, M., Schanzer, J., Croasdale, R., Dürr, H., Gassner, C., Georges, G., Kettenberger, H., Imhof-Jung, S., Schwaiger, M., Stubenrauch, K. G., Sustmann, C., Thomas, M., Scheuer, W., and Klein, C. (2011) Immunoglobulin domain crossover as a generic approach for the production of bispecific IgG antibodies. *Proc. Natl. Acad. Sci. U.S.A.* **108**, 11187–11192
- Gunasekaran, K., Pentony, M., Shen, M., Garrett, L., Forte, C., Woodward, A., Ng, S. B., Born, T., Retter, M., Manchulenko, K., Sweet, H., Foltz, I. N., Wittekind, M., and Yan, W. (2010) Enhancing antibody Fc heterodimer

## Applications to antibody production

- formation through electrostatic steering effects applications to bispecific molecules and monovalent IgG. *J. Biol. Chem.* **285**, 19637–19646
19. Ellerson, J. R., Yasmeen, D., Painter, R. H., and Dorrington, K. J. (1976) Structure and function of immunoglobulin domains III. Isolation and characterization of a fragment corresponding to the C $\gamma$ 2 homology region of human immunoglobulin G. *J. Immunol.* **116**, 510–517
  20. Ridgway, J. B., Presta, L. G., and Carter, P. (1996) 'Knobs-into-holes' engineering of antibody CH3 domains for heavy chain heterodimerization. *Protein Eng.* **9**, 617–621
  21. Ha, J. H., Kim, J. E., and Kim, Y. S. (2016) Immunoglobulin Fc heterodimer platform technology: from design to applications in therapeutic antibodies and proteins. *Front. Immunol.* **7**, 394
  22. Merchant, A. M., Zhu, Z., Yuan, J. Q., Goddard, A., Adams, C. W., Presta, L. G., and Carter, P. (1998) An efficient route to human bispecific IgG. *Nat. Biotechnol.* **16**, 677–681
  23. Gan, H. K., Burgess, A. W., Clayton, A. H., and Scott, A. M. (2012) Targeting of a conformationally exposed, tumor-specific epitope of EGFR as a strategy for cancer therapy. *Cancer Res.* **72**, 2924–2930
  24. Pedersen, M. W., Jacobsen, H. J., Koefoed, K., Hey, A., Pyke, C., Haurum, J. S., and Kragh, M. (2010) Sym004: A novel synergistic anti-epidermal growth factor receptor antibody mixture with superior anticancer efficacy. *Cancer Res.* **70**, 588–597
  25. Perera, R. M., Narita, Y., Furnari, F. B., Gan, H. K., Murone, C., Ahlqvist, M., Luwor, R. B., Burgess, A. W., Stockert, E., Jungbluth, A. A., Old, L. J., Cavenee, W. K., Scott, A. M., and Johns, T. G. (2005) Treatment of human tumor xenografts with monoclonal antibody 806 in combination with a prototypical epidermal growth factor receptor-specific antibody generates enhanced antitumor activity. *Clin. Cancer Res.* **11**, 6390–6399
  26. Jutten, B., Dubois, L., Li, Y., Aerts, H., Wouters, B. G., Lambin, P., Theys, J., and Lammering, G. (2009) Binding of cetuximab to the EGFRvIII deletion mutant and its biological consequences in malignant glioma cells. *Radiother. Oncol.* **92**, 393–398
  27. Fukai, J., Nishio, K., Itakura, T., and Koizumi, F. (2008) Antitumor activity of cetuximab against malignant glioma cells overexpressing EGFR deletion mutant variant III. *Cancer Sci.* **99**, 2062–2069
  28. Jungbluth, A. A., Stockert, E., Huang, H. J., Collins, V. P., Coplan, K., Iversen, K., Kolb, D., Johns, T. J., Scott, A. M., Gullick, W. J., Ritter, G., Cohen, L., Scanlan, M. J., Cavenee, W. K., Old, L. J., and Cavenee, W. K. (2003) A monoclonal antibody recognizing human cancers with amplification/overexpression of the human epidermal growth factor receptor. *Proc. Natl. Acad. Sci. U.S.A.* **100**, 639–644
  29. Jefferis, R. (2005) Glycosylation of recombinant antibody therapeutics. *Biotechnol. Prog.* **21**, 11–16
  30. Skartved, N. J., Jacobsen, H. J., Pedersen, M. W., Jensen, P. F., Sen, J. W., Jørgensen, T. K., Hey, A., and Kragh, M. (2011) Preclinical pharmacokinetics and safety of Sym004: a synergistic antibody mixture directed against epidermal growth factor receptor. *Clin. Cancer Res.* **17**, 5962–5972
  31. Baselga, J., and Swain, S. M. (2010) CLEOPATRA: a phase III evaluation of pertuzumab and trastuzumab for HER2-positive metastatic breast cancer. *Clin. Breast Cancer* **10**, 489–491
  32. Rasmussen, S. K., Naested, H., Müller, C., Tolstrup, A. B., and Frandsen, T. P. (2012) Recombinant antibody mixtures: production strategies and cost considerations. *Arch. Biochem. Biophys.* **526**, 139–145
  33. Ferrara, C., Grau, S., Jäger, C., Sondermann, P., Brünker, P., Waldhauer, I., Hennig, M., Ruf, A., Rufer, A. C., Stihle, M., Umaña, P., and Benz, J. (2011) Unique carbohydrate-carbohydrate interactions are required for high affinity binding between Fc $\gamma$ RIII and antibodies lacking core fucose. *Proc. Natl. Acad. Sci. U.S.A.* **108**, 12669–12674
  34. Nayak, S. U., Griffiss, J. M., McKenzie, R., Fuchs, E. J., Jura, R. A., An, A. T., Ahene, A., Tomic, M., Hendrix, C. W., and Zenilman, J. M. (2014) Safety and pharmacokinetics of XOMA 3AB, a novel mixture of three monoclonal antibodies against botulinum toxin A. *Antimicrob. Agents Chemother.* **58**, 5047–5053
  35. DeLano, W. L., Ultsch, M. H., de Vos, A. M., and Wells, J. A. (2000) Convergent solutions to binding at a protein-protein interface. *Science* **287**, 1279–1283
  36. Otwinowski, Z., and Minor, W. (1997) Processing of X-ray diffraction data collected in oscillation mode. *Methods Enzymol.* **276**, 307–326
  37. McCoy, A. J., Grosse-Kunstleve, R. W., Storoni, L. C., and Read, R. J. (2005) Likelihood-enhanced fast translation functions. *Acta Crystallogr. D Biol. Crystallogr.* **61**, 458–464
  38. McRee, D. E. (1999) XtalView/Xfit—A versatile program for manipulating atomic coordinates and electron density. *J. Struct. Biol.* **125**, 156–165
  39. Collaborative Computational Project No. 4. (1994) The CCP4 suite: programs for protein crystallography. *Acta Crystallogr. D Biol. Crystallogr.* **50**, 760–763
  40. Schrödinger, LLC (2015) The PyMOL Molecular Graphics System, Version 1.8, Schrödinger, LLC, New York

**A rational approach to enhancing antibody Fc homodimer formation for robust production of antibody mixture in a single cell line**

Jie Yu, Xiaoxiao Wang, Tao Xu, Qiheng Jin, Jinyuan Duan, Jie Wu, Haiyan Wu, Ting Xu and Sheng Ye

*J. Biol. Chem.* 2017, 292:17885-17896.

doi: 10.1074/jbc.M116.771188 originally published online September 6, 2017

---

Access the most updated version of this article at doi: [10.1074/jbc.M116.771188](https://doi.org/10.1074/jbc.M116.771188)

Alerts:

- [When this article is cited](#)
- [When a correction for this article is posted](#)

[Click here](#) to choose from all of JBC's e-mail alerts

Supplemental material:

<http://www.jbc.org/content/suppl/2017/09/06/M116.771188.DC1>

This article cites 39 references, 11 of which can be accessed free at <http://www.jbc.org/content/292/43/17885.full.html#ref-list-1>